Direct Detection of Singlet-Triplet Interconversion in OLED Magnetoelectroluminescence with a Metal-Free Fluorescence-Phosphorescence Dual Emitter

Wolfram Ratzke, Sebastian Bange,* and John M. Lupton
Institut für Experimentelle und Angewandte Physik, Universität Regensburg, Universitätsstrasse 31, 93053 Regensburg, Germany

(Received 10 November 2017; revised manuscript received 31 January 2018; published 25 May 2018)

We demonstrate that a simple phenazine derivative can serve as a dual emitter for organic light-emitting diodes, showing simultaneous luminescence from the singlet and triplet excited states at room temperature without the need of heavy-atom substituents. Although devices made with this emitter achieve only low quantum efficiencies of $< 0.2\%$, changes in fluorescence and phosphorescence intensity on the subpercent scale caused by an external magnetic field of up to 30 mT are clearly resolved with an ultra-low-noise optical imaging technique. The results demonstrate the concept of using simple reporter molecules, available commercially, to optically detect the spin of excited states formed in an organic light-emitting diode and thereby probe the underlying spin statistics of recombining electron-hole pairs. A clear anticorrelation of the magnetic-field dependence of singlet and triplet emission shows that it is the spin interconversion between singlet and triplet which dominates the magnetoluminescence response: the phosphorescence intensity decreases by the same amount as the fluorescence intensity increases. The concurrent detection of singlet and triplet emission as well as device resistance at cryogenic and room temperature constitute a useful tool to disentangle the effects of spin-dependent recombination from spin-dependent transport mechanisms.

DOI: 10.1103/PhysRevApplied.9.054038

I. INTRODUCTION

Even though the magnetic-field effect (MFE) of organic light-emitting diodes (OLEDs) has been investigated for many years, it is still difficult to pinpoint the underlying mechanisms [1–8]. In order to explain the change in the device resistance and luminescence, several models have been advanced which are based on the magnetic-field-dependent formation of singlet and triplet excited states or spin-dependent charge (polaron) transport channels [9–18]. Unfortunately, quantitative discrimination between them remains speculative as long as the role of spin-mixing processes is veiled in the absence of simultaneous experimental access to all three observables: singlet and triplet exciton yield, and device resistance. The two states of excitonic spin symmetry can be detected by measuring the fluorescence and phosphorescence, but so far this approach has been restricted to the exclusive observation of pure emission from either singlet *or* triplet states by investigating different molecular systems, and hence a coherent statement for one material is not possible [19–21]. This situation is attributed mainly to the lack of emitters exhibiting dual luminescence from singlet and triplet states. In order to observe dipole-forbidden phosphorescence the pure spin states have to be perturbed. The spin-orbit interaction (SOI) can introduce a mixing of spin states so that a dipole-allowed radiative decay within the same spin subspace becomes possible [22–29]. For the use of dual emitters as local probes of the spin state, it is crucial to achieve fluorescence and phosphorescence from the same molecule at comparable emission intensities and with minimal spectral overlap. Usually, the SOI is strongly enhanced by incorporating heavy atoms [30], an approach which is also known to perturb the molecule's immediate proximity and hence the actual molecular system of interest [31,32]. Incorporating trace amounts of covalently bound heavy atoms into polymeric materials offers one route to achieving sufficient spin-orbit coupling for the long-lived triplet state, but results in an inhomogeneous system that relies on triplet diffusion and cannot probe the pair process directly [33]. On the other hand, in organometallic emitters that directly incorporate the heavy atom, intersystem crossing is enhanced such that the singlet state is depleted and phosphorescence dominates the luminescence. In order to provide dual emission from a single chromophore, a compromise in the strength of the SOI and the transition dipole moments has to be found, implying that only molecules comprising light atoms with a low atomic number (low Z), i.e., hydrogen, carbon, nitrogen, and oxygen, can be used. Recently, we reported a range of thiophene-substituted phenazines as low-Z emitters which exhibit simultaneous

*Corresponding author.
sebastian.bange@ur.de

fluorescence and phosphorescence at room temperature by exploiting the highly localized action of the SOI operator on molecular orbitals of appropriate symmetry while suppressing the nonradiative decay rate [29,34]. Embedding such emitters into host matrices of OLEDs potentially offers a window to spin statistics by discriminating between spin-mixing mechanisms and other spin-dependent interactions which solely affect device resistance. Here, we demonstrate that a commercially available thiophene-free phenazine works equally well as a dual emitter, allowing us to visualize spin mixing in magnetic fields without having to resort to high-Z substituents [33].

II. EXPERIMENTAL SECTION

A. Photo- and electroluminescence

Bare phenazine is well known for its phosphorescence which is enabled by the lone-pair electrons of the nitrogen atoms [35–40]. However, phenazine is of limited use as an OLED dopant because the absorption is too far in the blue spectral region: carriers cannot be trapped on the dopant and back transfer of the triplet will occur to the matrix, quenching phosphorescence, so that it has not previously been considered as an OLED emitter. The simplest way to redshift the spectrum is by extending the conjugation path [29], e.g., as for the 11,12-dimethyldibenzo (a, c) phenazine (DMDB-PZ) investigated here, the structure of which is shown in the inset of Fig. 1(a).

The material was purchased from Sigma Aldrich and used without further purification. To measure photoluminescence (PL) spectra, shown in Fig. 1(a), the emitter is embedded in a poly(methyl-methacrylate) (PMMA, Sigma-Aldrich) matrix with a concentration of 3% by weight and excited at 370 nm. Under ambient conditions, the PL exhibits three features at 417, 432, and 464 nm, and a rather broad tail with a bump at 569 nm [Fig. 1(a), blue line]. The spectrum changes significantly when the measurement is performed under vacuum: a new emissive species arises in the red spectral region and the 569-nm feature becomes the dominant emission. This peak is assigned to phosphorescence of DMDB-PZ, which is quenched under ambient conditions by molecular oxygen. Further photophysical details of the material are given in the Supplemental Material [41–45].

OLEDs with DMDB-PZ as the emitter can be produced in different structures by either wet processing or by evaporation. The results presented here are obtained with a simple solution-processed device consisting of a poly (3,4-ethylene-dioxythiophene):poly(styrene-sulphonate) (PEDOT:PSS) hole-injection layer, an emitting layer of 4, 4′-bis (N-carbazolyl)-1, 1′-biphenyl (CBP) and DMDB-PZ with a ratio of 97∶3 by weight, and a barium and aluminum top electrode to give a pixel size of 4.2 mm^2. Details of the device preparation and the other device structures tested can be found in the Supplemental Material [41,46].

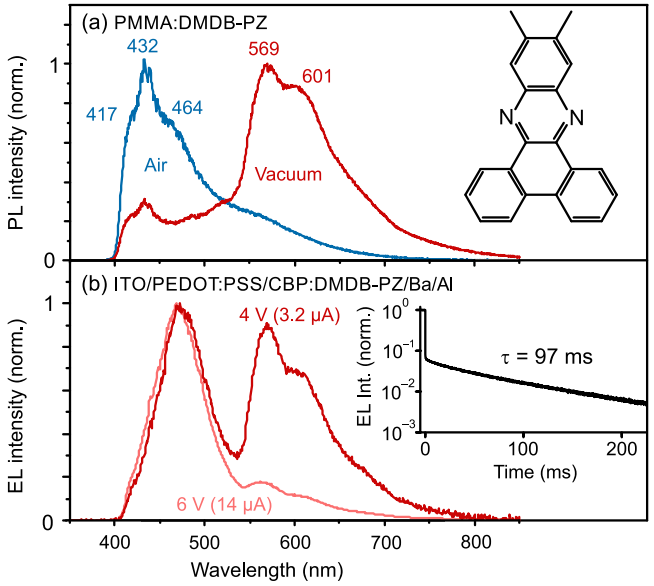

FIG. 1. (a) Room-temperature PL spectra of DMDB-PZ in PMMA as a thin film with a concentration of 3% by weight, excited at 370 nm. Under ambient conditions (blue line), the dominant luminescence occurs in the blue spectral region. A small bump is visible around 569 nm. Under vacuum (red line), the blue spectral components appear suppressed and the dominant emission arises in the red spectral region. Blue luminescence is attributed to singlet emission (fluorescence) and the red peak to phosphorescence from the triplet excited state. The inset shows the structure of the commercially available DMDB-PZ molecule. (b) EL spectra recorded at constant voltage under vacuum at room temperature. The triplet feature is strongly quenched with increasing driving power of the OLED. Spectrally integrated time-resolved EL after device switch-off is shown in the inset, demonstrating a triplet phosphorescence lifetime of 97 ms.

Room-temperature electroluminescence (EL) spectra of the device are shown in Fig. 1(b) for two different bias voltages. Again, two emissive species in the blue spectral region (464 nm) and the red (569 nm and 601 nm) are found. Here, the blue part is reminiscent of the PL spectrum measured under ambient conditions, as shown in Fig. 1(a), with reduced spectral structure and an effective redshift of the peak emission by 30 nm. The red region of the EL directly reproduces the triplet PL feature observed under vacuum conditions. The good match of the EL spectrum with the PL of the emitter indicates that emission from the OLEDs is neither due to exciplex formation nor due to the host matrix or any of the other molecular constituents. A decrease in the ratio between red and blue emission upon an increase of the bias voltage and current is attributed to quenching processes such as triplet-triplet or triplet-polaron annihilation [28]. Spectrally integrated delayed emission of the device as shown in the inset of panel (b) is measured as a function of time after switching the applied voltage from 6 to 0 V, using an avalanche photodiode with a time-correlated single-photon counting module for detection.

After an initial fast drop of this transient EL attributed to the singlet exciton species, the decay is single exponential as expected for monomolecular triplet exciton relaxation. The luminescence lifetime is 97 ms, the longest-lived triplet emission reported to date in an OLED. In previous work we investigated similar molecules where the phenyl rings were replaced by thiophenes [29]. Compared to these more complex emitters, one can see that the absence of sulfur atoms in the present case suppresses nonradiative decay, leading to a fourfold enhancement in triplet lifetime. The external quantum efficiency (EQE) of the device is determined by using an integrating sphere with a fiber-coupled spectrometer and found to be 0.003%. It is important to note that the detector used for the EQE measurement is less sensitive than that used for the EL spectra, so that the EQE could only be determined at a higher operating voltage than that used to measure the EL spectra. The EQE is, therefore, mainly related to the singlet emission and thus likely provides only an order-of-magnitude estimate of the lower bound of the device efficiency. As discussed in the Supplemental Material [41], the EQE is readily improved to 0.2% by alternative device stack layouts that improve charge balance.

B. Magnetic-field effect

In OLEDs, the uncorrelated injection of charges leads to a statistical distribution of singlet and triplet exciton precursor states, frequently referred to as polaron pairs [9]. However, as long as the recombination rates for singlet and triplet electron-hole pairs into molecular excited states differ slightly, spin mixing mediated by the hyperfine interaction can introduce an effective bias to the formation of singlet or triplet excited states [2,13]. Besides spin-dependent pair recombination and mixing, dissociation of the bound pairs into free carriers may also occur, a further potentially spin-dependent impact [47]. Predicting the effect of these processes in detail requires consideration of a stochastic Liouville approach [13,48] and ultimately also necessitates an understanding of the underlying hopping processes [44]. In addition, since our device is based on a blend system, carrier trapping effects may impact magnetoluminescence and magnetoresistance effects [49,50], complicating an *a priori* prediction of whether singlet or triplet yields should increase with an increasing magnetic field. However, since recombination is fundamentally spin dependent, the populations of singlet and triplet excitons, and thus fluorescence and phosphorescence, should anticorrelate as the magnetic field is varied. In order to not further complicate the investigation of the MFE we choose the device with the simplest layer design, which, however, also has the lowest EQE. The results therefore also demonstrate the remarkable overall sensitivity of the imaging-based measurement method described in the following.

1. Experimental setup

The device is mounted in an Oxford Instruments MicrostatHires2 pillared cryostat, with the cold mounting surface centered in a solenoid coil such that the magnetic field is aligned perpendicular to the device plane. The OLED is driven by a Keithley 236 source-measure unit at constant current, and the voltage is measured with a Keithley 2002 digital multimeter. A dichroic mirror (Semrock, 539 nm) is used to spatially separate fluorescence and phosphorescence into individual light paths, which are further spectrally isolated with 521-nm short-pass (Semrock) and 645-nm long-pass (Thorlabs) filters. The beams are then focused onto two separate areas of a thermoelectrically cooled, low-noise CMOS camera (Andor Zyla 4.2), where the two signals are individually integrated spatially to obtain their total intensities. In order to reduce the impact of device degradation on the measured field dependence, a total of typically 20 individual forward and backward sweeps of the magnetic field are used to calculate the average response. With the drift being approximately linear in time on the short time scale of individual sweeps, the averaging procedure effectively cancels out such effects, while at the same time improving the signal-to-noise ratio significantly. MFEs are readily observable for individual field sweeps, with camera exposure times of one second per data point, albeit at a higher noise level. A detailed discussion of data acquisition, processing, and evaluation including error estimates can be found in the Supplemental Material [41].

Prior magnetoresistance and magnetoelectroluminescence (MEL) experiments have mostly been performed under conditions of constant bias voltage. In such experiments, a change of the resistance causes a concomitant change of current and charge-carrier density in the OLED recombination zone. This change leads to an inherent correlation between electrical and optical observables and makes it impossible to distinguish between effects of spin-dependent charge transport and those related to the formation of excitonic states [5,12,51]. We therefore operate the OLED under conditions of constant drive current, probing the spin-dependent recombination process more selectively [11]. Constant-voltage magnetoresistance measurements are commonly performed precisely to give large magnetoresistance values. Note that due to the nonlinear OLED current-voltage characteristics, the magnetoresistance in constant current measurements is reduced by at least an order of magnitude [5] (see Supplemental Material for more details [41]). Another key aspect of sensitive MEL measurements is the method of light detection. The goal here is to provide maximum quantum efficiency for the detection of phosphorescence, which is usually weak, and at the same time ensure the highest possible sensitivity to small changes of the observable. Conventionally, either photomultipliers or photodiode systems have been employed in such measurements [3,6,8].

While photomultipliers are usually favored for extremely low-light-level applications due to their high gain, they suffer from poor noise characteristics, low quantum efficiency in the red spectral region, and are prone to spurious signals due to the experimental magnetic fields. On the other hand, silicon photodiodes with suitable transimpedance amplifiers usually provide low-noise signals but can only be used at sufficiently high photon flux. Modern scientific complementary metal-oxide (sCMOS) camera technology has advanced in recent years to make such detectors a surprisingly good choice for this application. Here, we rely on the detection quantum efficiency of over 80%, the low readout noise of around one electron per pixel, and the high signal-to-noise ratio which is limited mainly by the photon shot noise to $N/\sqrt{N}$, where N is the number of photoelectrons. Although each individual camera pixel is limited to 3×10^4 photoelectrons, signal-to-noise ratios near the shot-noise limit can be achieved in the crucial range of $N = 10^6 - 10^9$ after summing data from multiple pixels. This regime is out of reach both of sensitive photomultipliers and silicon avalanche photodiodes as well as low-noise silicon photodiodes operated in the photovoltaic mode. At the same time, sCMOS cameras provide large detector surfaces that facilitate optical coupling to large OLED device areas. A comprehensive signal-to-noise benchmark of the detection system can be found in the Supplemental Material [41].

2. Results and Discussion

Figure 2(a) shows the result of magnetoresistance and MEL measurements performed at a device current of 500 μA at room temperature. The changes relative to the value at zero field are plotted. Detailed electrical characterization of this device is provided in the Supplemental Material [41]. The change of singlet and triplet EL intensity is clearly anticorrelated and qualitatively follows a Lorentzian-type functionality $B^2/(B^2 + B_0^2)$ which has previously been reported for hyperfine-field-induced spin mixing [18], with similar linewidths B_0 of 6.5(1) and 6.0(4) mT for singlet and triplet, respectively (see Supplemental Material for all fit parameters [41]). We note that the high quality of the Lorentzian fit is likely related to the fact the MEL is obtained under conditions of constant current, which only probes spin-dependent recombination rather than transport effects. In contrast, the magnetoresistance is a hundredfold smaller than the MEL. Although it can clearly be described by a Lorentzian functionality for field magnitudes below 10 mT, the linewidth B_0 of 4.4(1) mT also appears to be narrower. Naturally, since the baseline of the Lorentzian is poorly defined, it is possible that B_0 in magnetoresistance is systematically underestimated. More reliably, the occurrence of additional turning points above ± 10 mT indicates a lack of direct correlation between magnetoresistance and MEL.

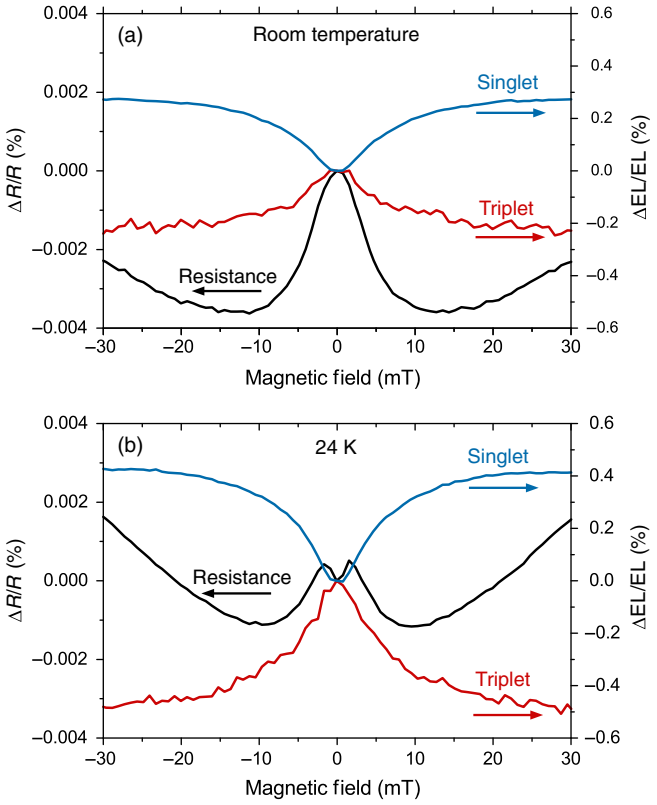

FIG. 2. (a) Simultaneous measurement of the relative magnetoresistance and the spectrally resolved relative MEL, separated into the singlet and triplet emission channels. The OLED is operated at room temperature and at a constant driving current of 500 μA. (b) The same device measured at 24 K with a current of 1000 μA. While singlet and triplet MEL are almost unaffected by the temperature change, an additional feature appears in the magnetoresistance at magnetic fields below 2 mT.

The measurement is repeated at a temperature of 24 K on the same device at a driving current of 1000 μA, as shown in Fig. 2(b). While the singlet and triplet MEL response is twice as strong compared to room temperature, the curve widths remain nearly identical. The central part of the magnetoresistance response, on the other hand, narrows and develops an additional feature within ± 2 mT. In prior reports, this ultrasmall magnetic-field effect has typically been seen in both (singlet) MEL and in magnetoresistance and is commonly attributed to stabilization of the spin state in the absence of the external magnetic field by weak exchange or spin-dipolar coupling [52–56]. Observing this response only in magnetoresistance and not in MEL implies that it cannot be directly caused by magnetic-field effects on the electron-hole pair exciton precursors, but is more likely related to the transport of charges towards the recombination zone. Studies of isotope effects on magnetoresistance and MEL in aluminum tris(8-hydroxyquinoline)-based devices suggest that magnetic-field-dependent interactions with triplet-state polaron pairs can indeed impact polaron transport without

contributing to singlet MEL [57,58], a process which will become more important at lower temperatures where triplets live longer.

The measurement results discussed in Fig. 2 are obtained by operating the OLEDs at rather high currents in order to increase the overall luminescence output and thus improve measurement sensitivity. At these operating conditions, quenching of triplet excitons due to triplet-triplet and triplet-polaron annihilation cannot be neglected and the singlet-triplet spectral ratio is typically skewed towards singlets when compared to the low-current situation depicted in Fig. 1. Triplet-triplet annihilation quenches triplet EL and could increase the population of singlet excitons [59], and thus might be expected to contribute to an anticorrelation of singlet and triplet electroluminescence. However, transient EL measurements (see Supplemental Material [41]) show no evidence of the delayed emission in the singlet channel expected from this process after switch-off of the device bias, indicating that such a mechanism cannot explain the reported singlet-triplet anticorrelation as a function of magnetic field. Additionally, spin-dependent transport due to the triplet-polaron interaction is known as an important contribution to the magnetoresponse of devices with unbalanced charge injection, particularly at low temperature [51,58]. The spin-dependent interaction between triplet excitons and polarons can, in principle, quench triplet excitons and impact conductivity due to scattering of the charge carriers. Pending an in-depth analysis of temperature and current dependence, we consider the complete absence of a correlation between magnetoresistance and both singlet and triplet MEL response curves though as good, if circumstantial evidence that the triplet-polaron interaction cannot explain the observed singlet-triplet anticorrelation in EL. We also note that the triplet-polaron interaction effect will have two distinct responses to the magnetic field, both due to the change in triplet density during recombination and due to the splitting of the triplet sublevels in the magnetic field. Finally, it should be stressed again that it is trivial to generate a correlation between MEL and magnetoresistance in measurements under constant-voltage bias, where the magnetoresistance explicitly determines the MEL. The fact that singlet and triplet EL both clearly roll off at room temperature and at the highest fields probed, whereas the resistance does not, demonstrates that EL indeed probes only spin-dependent recombination—which is determined solely by the local hyperfine field strengths—whereas the magnetoresistance does not, since it also includes spin-dependent transport effects which do not saturate as quickly.

III. SUMMARY

We demonstrate an imaging-based approach for MEL measurements of shot-noise limited sensitivity. Remarkably, a previously overlooked, commercially available material can serve as a low-Z dual emitter in OLEDs, enabling spin-resolved MEL detection. The approach constitutes a step towards directly resolving magnetic-field effects on spin-dependent recombination in OLEDs, and separating these from spin-dependent transport. Given the simplicity of the reporter molecules and the characteristic that they can be readily processed by both vacuum deposition as well as wet-chemical approaches, we expect that this approach can be generalized to other host materials. The fact that, over a ± 30-mT range the observed increase in fluorescence nearly perfectly matches the decrease in phosphorescence, at both room and low temperature, demonstrates that the underlying spin-mixing process responsible for magnetic-field effects is independent of temperature. This conclusion is in agreement with detailed studies of the temperature dependence of electrically detected magnetic resonance [11], and offers further constraints to parametrize stochastic models of organic magnetoresistance [48,52]. We note that a complete description of the magnetic-field effect would, in addition, require a consideration of both trapping effects and triplet-polaron spin-dependent transport effects. In future work, we expect to carry out a detailed analysis of the influence of macroscopic parameters, e.g., driving conditions, temperature, and device structure. Further, microscopic changes to the material including selective deuteration of parts of the emitter molecule as well as the CBP matrix to identify the spatial origin of hyperfine-field-induced spin mixing need to be addressed. Control over the emitter architecture will also allow us to probe the effect of the SOI on spin-mixing and spin-dependent transport. Finally, we note that these dual emitters provide a class of materials in between conventional singlet emitters and thermally activated delayed fluorescence emitters, which have been shown to exhibit extremely large magnetic-field effects of $>1000\%$ under constant-voltage conditions due to the formation of exciplexes [60,61]. It is an interesting question whether a suitable matrix can be found to prevent back transfer of both singlet and triplet excited states of the emitter while enabling the formation of exciplex species to enhance the overall magnetic-field response and thereby simplify optical detection of spin correlations further.

ACKNOWLEDGMENTS

The authors are indebted to the DFG for financial support through the SFB1277 project B3 as well as to Dr. Philippe Klemm for helpful discussions and Debra Daly for assistance in developing the device structures.

[1] K. Morgan and R. Pethig, Increase in d.c. dark conductivity of anthracene in a magnetic field, Nature (London) **213**, 900 (1967).

[2] J. Kalinowski, M. Cocchi, D. Virgili, P. Di Marco, and V. Fattori, Magnetic field effects on emission and current in Alq_3-based electroluminescent diodes, Chem. Phys. Lett. **380**, 710 (2003).

[3] A. H. Davis and K. Bussmann, Large magnetic field effects in organic light emitting diodes based on tris(8-hydroxyquinoline aluminum) (Alq_3)/N, N′-Di(naphthalen-1-yl)-N, N′ diphenyl-benzidine (NPB) bilayers, J. Vac. Sci. Technol. A **22**, 1885 (2004).

[4] M. Reufer, M. J. Walter, P. G. Lagoudakis, A. B. Hummel, J. S. Kolb, H. G. Roskos, U. Scherf, and J. M. Lupton, Spin-conserving carrier recombination in conjugated polymers, Nat. Mater. **4**, 340 (2005).

[5] Ö. Mermer, G. Veeraraghavan, T. L. Francis, and M. Wohlgenannt, Large magnetoresistance at room-temperature in small-molecular-weight organic semiconductor sandwich devices, Solid State Commun. **134**, 631 (2005).

[6] Y. Zhang, R. Liu, Y. L. Lei, and Z. H. Xiong, Low temperature magnetic field effects in Alq_3-based organic light emitting diodes, Appl. Phys. Lett. **94**, 083307 (2009).

[7] J. D. Bergeson, V. N. Prigodin, D. M. Lincoln, and A. J. Epstein, Inversion of Magnetoresistance in Organic Semiconductors, Phys. Rev. Lett. **100**, 067201 (2008).

[8] B. Hu and Y. Wu, Tuning magnetoresistance between positive and negative values in organic semiconductors, Nat. Mater. **6**, 985 (2007).

[9] E. L. Frankevich, A. A. Lymarev, I. Sokolik, F. E. Karasz, S. Blumstengel, R. H. Baughman, and H. H. Hörhold, Polaron-pair generation in poly(phenylene vinylenes), Phys. Rev. B **46**, 9320 (1992).

[10] H. Gu, X. Zhang, H. Wei, Y. Huang, S. Wei, and Z. Guo, An overview of the magnetoresistance phenomenon in molecular systems, Chem. Soc. Rev. **42**, 5907 (2013).

[11] M. Kavand, D. Baird, K. van Schooten, H. Malissa, J. M. Lupton, and C. Boehme, Discrimination between spin-dependent charge transport and spin-dependent recombination in π-conjugated polymers by correlated current and electroluminescence-detected magnetic resonance, Phys. Rev. B **94**, 075209 (2016).

[12] A. Buchschuster, T. D. Schmidt, and W. Brütting, Evidence for different origins of the magnetic field effect on current and electroluminescence in organic light-emitting diodes, Appl. Phys. Lett. **100**, 123302 (2012).

[13] S. P. Kersten, A. J. Schellekens, B. Koopmans, and P. A. Bobbert, Magnetic-Field Dependence of the Electroluminescence of Organic Light-Emitting Diodes: A Competition between Exciton Formation and Spin Mixing, Phys. Rev. Lett. **106**, 197402 (2011).

[14] V. N. Prigodin, J. D. Bergeson, D. M. Lincoln, and A. J. Epstein, Anomalous room temperature magnetoresistance in organic semiconductors, Synth. Met. **156**, 757 (2006).

[15] P. A. Bobbert, T. D. Nguyen, F. W. A. van Oost, B. Koopmans, and M. Wohlgenannt, Bipolaron Mechanism for Organic Magnetoresistance, Phys. Rev. Lett. **99**, 216801 (2007).

[16] S. Majumdar, H. S. Majumdar, H. Aarnio, D. Vanderzande, R. Laiho, and R. Österbacka, Role of electron-hole pair formation in organic magnetoresistance, Phys. Rev. B **79**, 201202 (2009).

[17] P. Desai, P. Shakya, T. Kreouzis, and W. P. Gillin, The role of magnetic fields on the transport and efficiency of aluminum tris(8-hydroxyquinoline) based organic light emitting diodes, J. Appl. Phys. **102**, 073710 (2007).

[18] Y. Sheng, T. D. Nguyen, G. Veeraraghavan, Ö. Mermer, M. Wohlgenannt, S. Qiu, and U. Scherf, Hyperfine interaction and magnetoresistance in organic semiconductors, Phys. Rev. B **74**, 045213 (2006).

[19] Y. Wu, Z. Xu, B. Hu, and J. Howe, Tuning magnetoresistance and magnetic-field-dependent electroluminescence through mixing a strong-spin-orbital-coupling molecule and a weak-spin-orbital-coupling polymer, Phys. Rev. B **75**, 035214 (2007).

[20] Y. Sheng, T. D. Nguyen, G. Veeraraghavan, Ö. Mermer, and M. Wohlgenannt, Effect of spin-orbit coupling on magnetoresistance in organic semiconductors, Phys. Rev. B **75**, 035202 (2007).

[21] J. Kalinowski, M. Cocchi, D. Virgili, V. Fattori, and P. Di Marco, Magnetic field effects on organic electrophosphorescence, Phys. Rev. B **70**, 205303 (2004).

[22] R. S. Becker, *Theory and Interpretation of Fluorescence and Phosphorescence* (Wiley Interscience, New York, 1969).

[23] C. M. Marian, Spin-orbit coupling and intersystem crossing in molecules, Comput. Mol. Sci. **2**, 187 (2012).

[24] D. S. McClure, Triplet-singlet transitions in organic molecules. lifetime measurements of the triplet state, J. Chem. Phys. **17**, 905 (1949).

[25] S. I. Weissman, Vector model for spin-orbit interaction in polyatomic molecules, J. Chem. Phys. **18**, 232 (1950).

[26] W. R. Wadt and W. A. Goddard, Electronic structure of pyrazine. Valence bond model for lone pair interactions, J. Am. Chem. Soc. **97**, 2034 (1975).

[27] D. S. McClure, Spin-orbit interaction in aromatic molecules, J. Chem. Phys. **20**, 682 (1952).

[28] A. Köhler and H. Bässler, Triplet states in organic semiconductors, Mater. Sci. Eng. R **66**, 71 (2009).

[29] W. Ratzke, L. Schmitt, H. Matsuoka, C. Bannwarth, M. Retegan, S. Bange, P. Klemm, F. Neese, S. Grimme, O. Schiemann, J. M. Lupton, and S. Höger, Effect of conjugation pathway in metal-free room-temperature dual singlet-triplet emitters for organic light-emitting diodes, J. Phys. Chem. Lett. **7**, 4802 (2016).

[30] H. Yersin, *Highly Efficient OLEDs with Phosphorescent Materials* (Wiley, Weinheim, 2007).

[31] M. Kasha, Collisional perturbation of spin-orbital coupling and the mechanism of fluorescence quenching. a visual demonstration of the perturbation, J. Chem. Phys. **20**, 71 (1952).

[32] D. F. Evans, E. Warhurst, and E. M. F. Roe, The effect of environment on singlet-triplet transitions of organic molecules [and discussion], Proc. R. Soc. A **255**, 55 (1960).

[33] H. Kraus, S. Bange, F. Frunder, U. Scherf, C. Boehme, and J. M. Lupton, Visualizing the radical-pair mechanism of molecular magnetic field effects by magnetic resonance induced electrofluorescence to electrophosphorescence interconversion, Phys. Rev. B **95**, 241201 (2017).

[34] D. Chaudhuri, E. Sigmund, A. Meyer, L. Röck, P. Klemm, S. Lautenschlager, A. Schmid, S. R. Yost, T. Van Voorhis, S. Bange, S. Höger, and J. M. Lupton, Metal-free OLED triplet emitters by side-stepping Kasha's rule, Angew. Chem., Int. Ed. **52**, 13449 (2013).

[35] K. Asano, S. Aita, and T. Azumi, Very weakly phosphorescent spin sublevels of phenazine. Mechanisms of

radiative and nonradiative transitions and the triplet-state geometry, J. Phys. Chem. **87**, 3829 (1983).
[36] A. J. Kallir, G. W. Suter, and U. P. Wild, Multiple phosphorescence of phenazine in ethanol at 77 K, J. Phys. Chem. **89**, 1996 (1985).
[37] T. G. Pavlopoulos, Vibronic spin orbit interaction in the phosphorescence spectrum of phenazine, J. Chem. Phys. **51**, 2936 (1969).
[38] B. Nickel and A. A. Ruth, Phosphorescence from phenazine in alkane solvents in the glass transition range: Spin-lattice, environment, and orientation relaxation of molecules in the metastable triplet state, J. Phys. Chem. **95**, 2027 (1991).
[39] Y. Hirata and I. Tanaka, Intersystem crossing to the lowest triplet state of phenazine following singlet excitation with a picosecond pulse, Chem. Phys. Lett. **43**, 568 (1976).
[40] J. P. Grivet and J. M. Lhoste, Electron spin resonance of triplet state phenazine, Chem. Phys. Lett. **3**, 445 (1969).
[41] See the Supplemental Material at http://link.aps.org/supplemental/10.1103/PhysRevApplied.9.054038 for further information on photophysical attributes of the emitter, details on device preparation, alternative device layer structures, quantum efficiencies, time-gated EL spectra, data acquisition for magnetoresistance and MEL and averaging procedure, noise levels, and difference in device bias type.
[42] A. T. R. Williams, S. A. Winfield, and J. N. Miller, Relative fluorescence quantum yields using a computer-controlled luminescence spectrometer, Analyst **108**, 1067 (1983).
[43] W. H. Melhuish, Quantum efficiencies of fluorescence of organic substances: effect of solvent and concentration of the fluorescent solute, J. Phys. Chem. **65**, 229 (1961).
[44] C. A. Richard, Z. Pan, H.-Y. Hsu, S. Cekli, K. S. Schanze, and J. R. Reynolds, Effect of isomerism and chain length on electronic structure, photophysics, and sensitizer efficiency in quadrupolar $(\text{donor})_2$-acceptor systems for application in dye-sensitized solar cells, ACS Appl. Mater. Interfaces **6**, 5221 (2014).
[45] Y. J. Lei, J. Ouyang, and M. Ding, Synthesis and spectroscopic properties of 2-(7-fluoro-1H-imidazo[4,5-B]phenazin-2-Yl)-phenol derivatives, Adv. Mater. Res. **287–290**, 2057 (2011).
[46] G. Liu, J. B. Kerr, and S. Johnson, Dark spot formation relative to ITO surface roughness for polyfluorene devices, Synth. Met. **144**, 1 (2004).
[47] D. R. McCamey, S. Y. Lee, S. Y. Paik, J. M. Lupton, and C. Boehme, Spin-dependent dynamics of polaron pairs in organic semiconductors, Phys. Rev. B **82**, 125206 (2010).
[48] F. Macia, F. Wang, N. J. Harmon, A. D. Kent, M. Wohlgenannt, and M. E. Flatté, Organic magnetoelectroluminescence for room temperature transduction between magnetic and optical information, Nat. Commun. **5**, 3609 (2014).
[49] M. Cox, P. Janssen, F. Zhu, and B. Koopmans, Traps and trions as origin of magnetoresistance in organic semiconductors, Phys. Rev. B **88**, 035202 (2013).
[50] N. J. Harmon and M. E. Flatté, Organic magnetoresistance from deep traps, J. Appl. Phys. **116**, 043707 (2014).
[51] P. Desai, P. Shakya, T. Kreouzis, W. P. Gillin, N. A. Morley, and M. R. J. Gibbs, Magnetoresistance and efficiency measurements of Alq_3-based OLEDs, Phys. Rev. B **75**, 094423 (2007).
[52] A. J. Schellekens, W. Wagemans, S. P. Kersten, P. A. Bobbert, and B. Koopmans, Microscopic modeling of magnetic-field effects on charge transport in organic semiconductors, Phys. Rev. B **84**, 075204 (2011).
[53] T. D. Nguyen, B. R. Gautam, E. Ehrenfreund, and Z. V. Vardeny, Magnetoconductance Response in Unipolar and Bipolar Organic Diodes at Ultrasmall Fields, Phys. Rev. Lett. **105**, 166804 (2010).
[54] T. D. Nguyen, G. Hukic-Markosian, F. Wang, L. Wojcik, X.-G. Li, E. Ehrenfreund, and Z. V. Vardeny, Isotope effect in spin response of π-conjugated polymer films and devices, Nat. Mater. **9**, 345 (2010).
[55] P. Klemm, S. Bange, A. Pöllmann, C. Boehme, and J. M. Lupton, Nanotesla magnetoresistance in π-conjugated polymer devices, Phys. Rev. B **95**, 241407 (2017).
[56] N. J. Harmon and M. E. Flatté, Effects of spin-spin interactions on magnetoresistance in disordered organic semiconductors, Phys. Rev. B **85**, 245213 (2012).
[57] T. D. Nguyen, T. P. Basel, Y.-J. Pu, X.-G. Li, E. Ehrenfreund, and Z. V. Vardeny, Isotope effect in the spin response of aluminum tris(8-hydroxyquinoline) based devices, Phys. Rev. B **85**, 245437 (2012).
[58] W. J. Baker, D. R. McCamey, K. J. van Schooten, J. M. Lupton, and C. Boehme, Differentiation between polaron-pair and triplet-exciton polaron spin-dependent mechanisms in organic light-emitting diodes by coherent spin beating, Phys. Rev. B **84**, 165205 (2011).
[59] C. Rothe, R. Guentner, U. Scherf, and A. P. Monkman, Trap influenced properties of the delayed luminescence in thin solid films of the conjugated polymer Poly (9,9-di(ethylhexyl)fluorene), J. Chem. Phys. **115**, 9557 (2001).
[60] T. Basel, D. L. Sun, S. Baniya, R. McLaughlin, H. Choi, O. Kwon, and Z. V. Vardeny, Magnetic field enhancement of organic light-emitting diodes based on electron donor-acceptor exciplex, Adv. Electron. Mater. **2**, 1500248 (2016).
[61] Y. F. Wang, K. Sahin-Tiras, N. J. Harmon, M. Wohlgenannt, and M. E. Flatté, Immense Magnetic Response of Exciplex Light Emission due to Correlated Spin-Charge Dynamics, Phys. Rev. X **6**, 011011 (2016).